

THE ESA HUYGENS PROBE ENTRY AND DESCENT TRAJECTORY RECONSTRUCTION

B. Kazeminejad¹ and D.H. Atkinson²

¹Space Research Institute (IWF), Austrian Academy of Sciences, Schmiedlstr. 6, A-8042 Graz, Austria

²Dept. of Electrical and Computer Engineering, University of Idaho, Moscow ID-83844-1023, USA

ABSTRACT

Cassini/Huygens is a joint NASA/ESA mission on its way to explore the Saturnian system. The ESA Huygens probe is scheduled to be released from the Cassini spacecraft on December 25, 2004, will enter the atmosphere of Titan in January, 2005, and will descend to the surface of the planet using a sequence of different parachutes. To correctly interpret and correlate results from the probe science experiments and to provide a reference set of data for “ground-truthing” Orbiter remote sensing measurements, it is essential that the trajectory reconstruction be performed as early as possible in the post-flight data analysis phase. The reconstruction of the Huygens entry and descent trajectory will be based primarily on the probe entry state vector provided by the Cassini Navigation Team, and measurements of acceleration, pressure, and temperature made by the Huygens Atmospheric Structure Instrument (HASI). Other datasets contributing to the entry and descent trajectory reconstruction include the mean molecular weight of the atmosphere measured by the probe Gas Chromatograph/Mass Spectrometer (GCMS) in the upper atmosphere and the Surface Science Package (SSP) speed of sound measurement in the lower atmosphere, and probe altitude by the two probe radar altimeters during the latter stages of the descent. Measurements of the zonal wind drift by the Doppler Wind Experiment (DWE), and probe zonal and meridional drift, and probe altitude and descent speed by the Descent Imager and Spectral Radiometer (DISR) will further constrain the probe trajectory. This paper outlines the mathematical approach and computational flow of an algorithm that combines all the relevant measurements to retrieve the probe trajectory most consistent with all data sets, and the probe trajectory uncertainties.

Key words: Huygens mission, trajectory reconstruction.

1. INTRODUCTION

1.1. Probe Mission Overview

The Huygens Probe is the ESA-provided element of the joint NASA/ESA/ASI Cassini/Huygens mission

to Saturn and Titan (Lebreton and Matson, 2002). Cassini/Huygens was launched on October 15, 1997 and is scheduled to arrive at Saturn on July 1, 2004. Following two orbits of Saturn, the Huygens Probe will be released on December 25, 2004 and will reach Titan on January 14, 2005.

The Huygens probe carries six instruments that will perform scientific measurements of the physical and chemical properties of Titan’s atmosphere, measure winds and global temperatures, and investigate energy sources important for the planet’s chemistry throughout the descent mission. These instruments are

- Aerosol Collector and Pyrolyser (ACP) (Israel *et al.*, 1997)
- Atmospheric Structure Instrument (HASI) (Fulchignoni *et al.*, 1997)
- Descent Imager/Spectral Radiometer (DISR) (Tomasko *et al.*, 1997)
- Doppler Wind Experiment (DWE) (Bird *et al.*, 1997)
- Gas Chromatograph and Mass Spectrometer (GCMS) (Niemann *et al.*, 1997)
- The Surface Science Package (SSP) (Zarnecki *et al.*, 1997)

It is expected that the probe will survive impact, so a sixth experiment, the Surface Science Package, has been included to perform for an investigation of the physical and chemical properties of Titan’s surface. All of Huygens’ entry and descent science and engineering data will be transmitted to the Cassini Orbiter, targeted to flyby Titan at a periapse distance of 60,000 km, where it will be recorded for later transmission to Earth.

1.2. Huygens Probe Descent Mission

The Huygens probe is protected from the atmospheric induced radiative and convective heat fluxes during entry

by a 2.75 meter diameter front heat-shield as it decelerates from about Mach 22.5 to Mach 1.5 in just under five minutes. Approximately 4.5 minutes after entry the probe speed will have decreased to Mach 1.5 and the probe Central Acceleration Sensor Unit (CASU) will measure the deceleration threshold designated as S_0 . At S_0 the entry portion of the mission is complete and the descent mission commences.

Approximately 6.375 seconds after S_0 a parachute deployment device is fired through a breakout patch in the aft cover of the probe and a 2.59 m disk gap band (DGB) type pilot parachute is deployed. Two and one half seconds later, the aft cover is released and the 8.3 meter main DGB parachute is deployed. Nominally this event occurs at Mach 1.5 and an altitude of 160 km. After a 30 second delay (built into the sequence to ensure that the shield is sufficiently far below the probe to avoid possible instrument contamination), the probe speed has dropped to Mach 0.6 and the inlet ports of the probe Gas Chromatograph/Mass Spectrometer and Aerosol Collector and Pyrolyser instruments are opened and the booms of the Huygens Atmospheric Structure Instrument deployed.

The probe will descend beneath the main parachute for 15 minutes, at which time the main parachute is released and a 3.03 meter drogue parachute is deployed to carry the probe to Titan's surface. Throughout the approximately 2.5 hour parachute descent to the surface, Huygens will measure the chemical, meteorological, and dynamical properties of the Titan atmosphere. Probe experiment and housekeeping/engineering data will be transmitted to the orbiter at 8 kbit/s.

1.3. Need for a Consistent Entry and Descent Trajectory

For a consistent interpretation and correlation of results from all the probe science experiments, and to provide confidence in ground-truth calibrations of orbiter remote sensing measurements, an accurate reconstruction of the probe entry and descent trajectory is needed. Without a common and consistent descent profile, each probe experiment team would need to develop a profile independently thereby causing a significant duplication of effort and expenditure of resources, and making correlation and comparison of results from different experiments somewhat suspect and therefore less meaningful. Furthermore, direct (*in situ*) atmospheric sampling by the probe will provide "ground truth" verification of orbiter observations of Titan. Without a means to tie the measured atmospheric properties to the probe altitude, location, and velocity at specific times, the value of ground-truth support for orbiter science at Titan would be significantly compromised.

The goals of the Huygens trajectory reconstruction effort are therefore

1. to provide a common trajectory for all experiment teams to use when interpreting their respective data sets. This will also eliminate the need for each team

to perform the task independently and thereby offering a more economical use of limited resources;

2. to provide a common basis for interpretation and correlation of data from different experiments. For example, the existence of atmospheric turbulence and wind shear, evident from the unique signatures in the HASI accelerometer data can only be correlated with other atmospheric properties such as temperature gradients, winds, and cloud decks if a common probe trajectory profile is utilized by all the experiment teams;
3. to provide the atmospheric properties along the probe entry and descent path for use by the orbiter experiment teams as a means of "ground-truthing" remote sensing measurements;
4. to provide precise measurements of the probe position and velocity throughout descent, required for the DWE recovery of the zonal winds by Doppler tracking of the Huygens probe.

1.4. Huygens Descent Trajectory Working Group (DTWG)

The responsibility of developing analysis techniques by which the Huygens entry and descent trajectory will be reconstructed from the the official NASA/ESA hand-off point at the interface altitude of 1270 km to the surface is given to the Huygens Descent Trajectory Working Group (DTWG), chartered in 1996 as a subgroup of the Huygens Science Working Team (HSWT) (Atkinson, 1998). The membership of the DTWG includes the Huygens and Cassini project scientists, the Huygens Operations Scientist, and representatives from each of the probe science instrument teams and contributing orbiter teams. The primary goals of the Descent Trajectory Working Group are

- to develop a framework between experiment teams and the Huygens Mission Team for sharing and exchanging data relevant to the descent trajectory analysis and modeling;
- to develop methodologies by which the probe descent trajectory and attitude can be accurately reconstructed from the probe and orbiter science and engineering data; and
- to provide a single, common descent profile that is consistent with all the available probe and orbiter engineering and science data, and that can be utilized by each instrument team for analysis of experiment measurements, and correlation of results between experiments.

2. PROBE INITIAL CONDITIONS AT INTERFACE ALTITUDE

The Huygens probe is scheduled to arrive at the entry interface point at 9:00:00 TDB on 14 January 2005. The

interface point is designated to be at an altitude 1270 km above the surface of Titan, a west longitude of 186.19 degrees, and a latitude of 9.525 degrees South. The Cassini Navigation team will provide to the DTWG the full state vector (i.e., position and velocity) of the Huygens Probe at the interface point in a Titan-centered EME2000 coordinate system together with associated uncertainties in the form of a covariance matrix.

2.1. Probe Imaging

Following the probe release, the Cassini cameras will attempt to image the probe as it begins its 21 day coast to Titan. The purpose of probe imaging is to apply optical navigation techniques to improve the knowledge of probe delivery to the interface point. The probe images (opnavs) will be unable to improve probe delivery accuracies (D. Roth, private communication), however, since the images are to be obtained after separation after which there is no longer an opportunity to affect the probes trajectory. However, opnavs will improve estimates of the post-separation probe trajectory and therefore decrease the delivery dispersion ellipse at the NASA/ESA interface point.

There are three imaging opportunities, one each day between probe release and the Orbiter Deflection Maneuver (ODM). The strategy is to attempt to image the probe by taking a 5×5 mosaic on either the first or second day through the Wide Angle Camera (WAC). Assuming the probe is located in the images, a subsequent image would be taken on the second or third day using the Narrow Angle Camera (NAC). On the first day, the probe image could be as large as 3-9 pixels across through the WAC, dropping to less than 2 pixels on the second day. With a focal length $10\times$ that of the WAC, the NAC would provide an image of the probe that is 15 pixels across on the second day (approximately release + 30 hours), and 8 pixels across on the third day (release + 55 hours).

The benefit of probe optical navigation is to significantly improve (i.e., reduce) the (1σ) delivery uncertainties. With imaging, the probe 1σ delivery dispersion error improves in the radial direction from 73.12 km to 42.80 km, along the B-plane semi-major axis from 58.24 km to 27.24 km, and along the B-plane semi-minor axis from 9.37 km to 5.77 km.

3. RECONSTRUCTION OF THE REFERENCE TRAJECTORY

The general computational flow of the full DTWG reconstruction algorithm is outlined in Fig. 1. In theory, the probe trajectory can be fully determined from the measured aerodynamic forces from the onboard accelerometers (i.e., HASI 3-axis science accelerometers and the 1-axis accelerometer from the Central Acceleration Sensor Unit (CASU)) and knowledge of the probe state vector at a given starting point. The gravitational force acting on the spacecraft's center of mass cannot be detected by measurements made in a frame fixed with respect to the

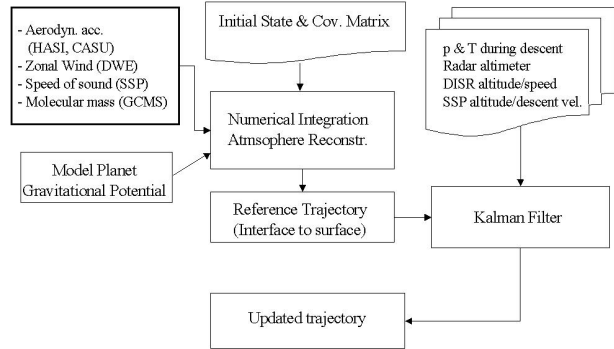


Figure 1. General flow of the Huygens probe reconstruction algorithm.

spacecraft, since the spacecraft and the accelerometer instrument are both free falling at the same rate. This force has therefore to be modelled at each step of the reconstruction process. During the probe entry phase (defined as the portion of the trajectory from interface altitude to the initiation of the parachute sequence at ~ 160 km) only accelerations are measured by the probe instruments. The deployment of the parachute will most likely introduce some oscillatory motions into the spacecraft, and hence into the the measured accelerations as well, as it swings around on the end of its parachute. A probe trajectory that is based entirely on the numerical integration of the measured and calculated accelerations (this trajectory is referred to as the “reference trajectory”) will generally deviate from the actual spacecraft trajectory. This trajectory must therefore be updated using further input data that can constrain the probe position and velocity during the descent phase. These additional data sets will come from the HASI atmospheric pressure and temperature sensors (which must be converted into an altitude and descent speed), the two radar units (RAU1 and RAU2), the SSP acoustic sounder instrument, and from the DISR images that can be processed to yield a probe position and descent velocity. A sequential estimation algorithm (i.e., a Kalman filter) will be implemented to update the reference trajectory and provide a “best combination” of all available data sets.

3.1. The Numerical Integration of the Accelerometer Data

To reconstruct a probe's entry and descent trajectory, the equations of motion are traditionally formulated and integrated in a rotating, planet-fixed coordinate frame. For the Huygens reconstruction, the added complexity of including the Coriolis and centrifugal forces has been eliminated by integrating the equations of motion in the inertial planet-centered Earth Mean Equator and equinox of J2000 (EME2000) frame.

In the framework of Newtonian physics the acceleration of a satellite \mathbf{a} under the influence of a force \mathbf{F} is described by the differential equation

$$\mathbf{a} = \ddot{\mathbf{r}} = \mathbf{F}(t, \mathbf{r}, \mathbf{v})/m \quad (1)$$

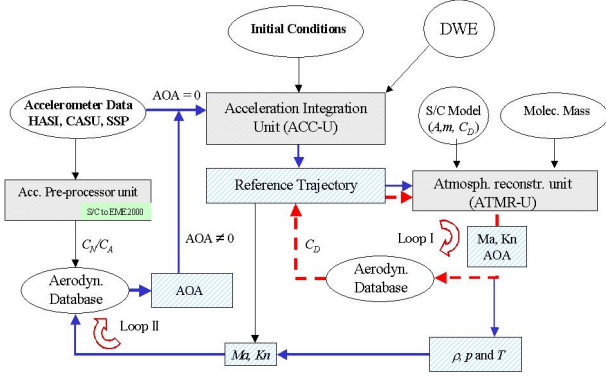


Figure 2. Detailed computational flow diagram of the Reference Trajectory reconstruction part of the DTWG algorithm. There are two internal iteration loops that need to converge: Loop I to interpolate the drag coefficient C_D and Loop II to apply the derived angle of attack (AOA) in the conversion of the accelerations from S/C frame to the integration frame. See text for detailed explanation.

where \mathbf{r} and $\mathbf{v}(= \dot{\mathbf{r}})$ are the position and velocity vectors of the body in a planet centered (inertial) coordinate system, and m denotes the mass of the spacecraft. For an atmospheric entry probe we have to consider mainly two types of acceleration that will determine its trajectory: an acceleration due to the gravitational attraction of the primary and secondary (perturbing) planets, \mathbf{a}_g , and an acceleration due to the aerodynamic forces produced by the atmosphere of the primary planet, \mathbf{a}_{Ad} . Eq. (1) can therefore be rewritten as

$$\mathbf{a} = \mathbf{a}_g + \mathbf{a}_{Ad} = \ddot{\mathbf{r}} = \mathbf{F}(t, \mathbf{r}, \mathbf{v})/m \quad (2)$$

The gravitational acceleration \mathbf{a}_g of a spacecraft due to the primary point mass M_0 (e.g., Titan in our special case) and N perturbing masses (e.g., the Sun and Saturn) in the planet centered EME2000 coordinate system is given by

$$\mathbf{a}_g = -G M_0 \frac{\mathbf{r}}{|\mathbf{r}|^3} + \sum_{j=1}^n G M_j \left[\frac{\mathbf{p}_j - \mathbf{r}}{|\mathbf{p}_j - \mathbf{r}|^3} - \frac{\mathbf{p}_j}{|\mathbf{p}_j|^3} \right] + \nabla U \quad (3)$$

where \mathbf{r} and \mathbf{p}_j are the position vectors of the spacecraft and the j th perturbing body ($j = 1..n$) respectively, G the gravitational constant, and ∇U the gradient of the disturbing function due to the dynamical flattening of the planet (axisymmetric gravity field assumed) which is given by

$$U = G M_0 \sum_{k=2}^{\infty} J_k \frac{R_P^k}{|\mathbf{r}|^{k+1}} P_k(\sin \Theta) . \quad (4)$$

R_P is the equatorial radius of the planet, Θ the latitude of the spacecraft above the planet's equatorial plane, and J_k the coefficient of the k th zonal harmonic. P_k is the Legendre polynomial of degree k . The spherical latitude Θ

can be calculated from the r'_3 component of the probe position vector in the so called Equatorial Coordinate System (defined by the coordinates $\mathbf{r}' = (r'_1, r'_2, r'_3)$)¹

$$r'_3 = |\mathbf{r}| \sin \Theta \quad (5)$$

Using

$$\mathbf{r}' = \mathbf{E} \mathbf{r} \quad (6)$$

where \mathbf{E} is a rotation matrix given by

$$\mathbf{E} = \begin{pmatrix} -\sin \alpha_0 & \cos \alpha_0 & 0 \\ -\cos \alpha_0 \sin \delta_0 & -\sin \alpha_0 \sin \delta_0 & \cos \delta_0 \\ \cos \alpha_0 \cos \delta_0 & \sin \alpha_0 \cos \delta_0 & \sin \delta_0 \end{pmatrix} \quad (7)$$

$\sin \Theta$ can equally be expressed in EME2000 coordinates $\mathbf{r} = (r_1, r_2, r_3)$:

$$\begin{aligned} \sin \Theta &= \frac{r'_3}{|\mathbf{r}|} = \\ &= \frac{1}{|\mathbf{r}|} (r_1 \cos \alpha_0 \cos \delta_0 + r_2 \sin \alpha_0 \cos \delta_0 + \\ &\quad + r_3 \sin \delta_0) \end{aligned} \quad (8)$$

It can now be seen that

$$\begin{aligned} \frac{\partial \sin \Theta}{\partial r_1} &= -\frac{\sin \Theta r_1}{|\mathbf{r}|^2} + \frac{\cos \delta_0 \cos \alpha_0}{|\mathbf{r}|} \\ \frac{\partial \sin \Theta}{\partial r_2} &= -\frac{\sin \Theta r_2}{|\mathbf{r}|^2} + \frac{\cos \delta_0 \sin \alpha_0}{|\mathbf{r}|} \\ \frac{\partial \sin \Theta}{\partial r_3} &= -\frac{\sin \Theta r_3}{|\mathbf{r}|^2} + \frac{\sin \delta_0}{|\mathbf{r}|} \end{aligned} \quad (9)$$

where α_0 and δ_0 are the right ascension and declination of the planet's north pole. With the Legendre polynomial $P_2(x)$ given by

$$P_2(x) = \frac{3}{2}x^2 - \frac{1}{2} \quad (10)$$

∇U in Eq. (3) developed to degree 2 becomes

¹The Equatorial System is introduced by rotating the coordinate axes of the EME2000 system by $90^\circ - \delta_0$ around x-axis and $\alpha_0 + 90^\circ$ about the z axis, where α_0 and δ_0 are the right ascension and declination of the planet's north pole. In that Equatorial system the x' axis points to the intersection of the earth mean equator of the epoch J2000 and the planet's equator, the z' axis points to the planet's north pole (and is parallel with its rotation axis), and y' axis fills out an orthogonal right-handed system. The Equatorial System is an inertial (i.e., non rotating) system.

$$\begin{aligned}
\frac{\partial U}{\partial r_1} &= \kappa \left\{ \frac{r_1}{|\mathbf{r}|^5} \chi(\Theta) - \frac{3}{|\mathbf{r}|^4} \sin \Theta \cos \alpha_0 \cos \delta_0 \right\} \\
\frac{\partial U}{\partial r_2} &= \kappa \left\{ \frac{r_2}{|\mathbf{r}|^5} \chi(\Theta) - \frac{3}{|\mathbf{r}|^4} \sin \Theta \sin \alpha_0 \cos \delta_0 \right\} \\
\frac{\partial U}{\partial r_3} &= \kappa \left\{ \frac{r_3}{|\mathbf{r}|^5} \chi(\Theta) - \frac{3}{|\mathbf{r}|^4} \sin \Theta \sin \delta_0 \right\} \quad (11)
\end{aligned}$$

where κ is a constant given by

$$\kappa = G M_0 J_2 R_p^2 \quad (12)$$

and χ a function defined by

$$\chi(x) = \left(\frac{15}{2} \sin^2 x - \frac{3}{2} \right) \quad (13)$$

The aerodynamic force acceleration vector can be directly deduced by interpolation of the measured linear accelerations of the spacecraft center of mass in the three orthogonal directions a_{s1}, a_{s2}, a_{s3} aligned with the spacecraft $s_1, s_2,$ and s_3 axes, respectively. The correct transformation of the accelerations measured in the spacecraft frame (s_1, s_2, s_3) to the inertial frame requires the knowledge of the orientation of the spacecraft attitude with respect to the direction of the flow velocity (given in the inertial frame of integration). This is expressed by the angle of attack $\alpha(t)$. The angle of attack can be estimated using the ratio of normal to axial accelerations

$$\frac{a_N}{a_A} = \frac{C_N}{C_A} = f(\alpha, Ma) \quad (14)$$

where a_N and a_A are the normal and axial accelerations given by $a_N = \sqrt{a_{s2}^2 + a_{s3}^2}$ and $a_A = a_{s1}$ respectively, and C_N and C_A are the corresponding aerodynamic coefficients. An existing pre-flight aerodynamic database of the Huygens probe (P. Couzin, private communication) provides C_N and C_A as a function of α and the Mach number Ma . From the normal and axial accelerations a_N and a_A , the angle of attack α can be found by interpolating the aerodynamic database. The drag and lift accelerations a_D and a_L can then be found from

$$\begin{aligned}
a_D &= a_A \cos \alpha + a_N \sin \alpha \\
a_L &= a_N \cos \alpha - a_A \sin \alpha \quad (15)
\end{aligned}$$

where, again, $a_N = \sqrt{a_{s2}^2 + a_{s3}^2}$ and $a_A = a_{s1}$.

Due to probe spin the lift force vector will rotate with the probe and average to zero (assuming the lift force is essentially constant over a spin period) and can therefore be neglected. The drag force vector \mathbf{a}_{Ad} is always pointing in the opposite direction of the relative flow velocity vector \mathbf{v}_{rel} of the spacecraft with respect to the fluid (i.e., the

atmosphere) in the inertial frame of integration and can be found from

$$\mathbf{a}_{Ad} = -a_D \frac{\mathbf{v}_{rel}}{|\mathbf{v}_{rel}|} \quad (16)$$

and \mathbf{v}_{rel} can be calculated using the relation

$$\mathbf{v}_{rel} = \mathbf{v} - \omega_p \times \mathbf{r} - \mathbf{v}_w \quad (17)$$

where \mathbf{r} and \mathbf{v} are the probe position and velocity vectors in the inertial frame, ω_p is the angular velocity vector of the planet, and \mathbf{v}_w the velocity vector of the atmospheric wind. As can be seen from Eq. (17) the probe entry and descent trajectory depends upon the atmospheric winds. Likewise the DWE retrieval algorithm depends strongly upon the accurate knowledge of the probe terminal entry and descent location (latitude and longitude). The need for a precise wind profile to accurately model the probe descent trajectory, and the need for a well developed probe entry and descent profile to retrieve zonal winds suggests the trajectory recovery analysis will be an iterative process.

3.2. Reconstruction of Atmospheric Properties from Accelerometer Data

The calculation of the Mach number in Eq. (14) requires the atmospheric temperature T and molecular weight μ to be known,

$$Ma = \frac{|\mathbf{v}_{rel}|}{c_s} \quad (18)$$

where \mathbf{v}_{rel} is the relative velocity between the spacecraft and the atmosphere (see Eq. (17)) and c_s is the speed of sound given by

$$c_s = \sqrt{\frac{\gamma R T}{\mu}} \quad (19)$$

γ is the ratio of specific heats, and $R = 8.314 \text{ J K}^{-1} \text{ mol}^{-1}$ is the universal gas constant. Note that neither T nor μ are directly measured during the entry phase. The relative abundance of methane and argon will vary with altitude in the upper atmosphere because of diffusive separation but should be constant at altitudes below 600 km (Yelle *et al.*, 1997). In the upper atmosphere the molecular weight can be modelled using analytic expressions for the methane and argon mole fractions as a function of altitude (Strobel *et al.*, 1992; Steiner and Bauer, 1990). The CH_4 mole fraction is calculated from

$$f_{CH_4} = A_1 \left(1 + e^{(1-\nu)h} \right)^{\frac{3}{7(1-\nu)}} + A_2 \quad (20)$$

and the Argon mole fraction from

$$f_{Ar} = A_3 \left(1 + e^{(1-\nu)h} \right)^{\frac{-0.3}{(1-\nu)}} \quad (21)$$

where h is the normalized geopotential height measured relative to the homopause

$$h = 1.67 \times 10^5 \frac{z - z_H}{(R_T + z_H)(R_T + z)} \quad (22)$$

z_H defines the altitude of the homopause and R_T the radius of Titan. A_1 , A_2 , and A_3 are integration constants used to match conditions deep in the atmosphere. The parameter ν describes the altitude of the eddy diffusion coefficient. Yelle *et al.* (1997) provides the following values for his recommended Titan atmosphere model: ν , A_1 , A_2 , A_3 , and z_H are 0.625, 0.240, 0.006, 0.020, and 1050.0 km respectively. The molecular weight of the gas mixture can then be calculated from

$$\mu = \sum_i f_i \mu_i \quad (23)$$

where μ_i is the molecular weight of the species i with the mole fraction f_i .

During the descent phase (i.e., the altitude range from ~ 160 km down to the surface) the mean molecular mass μ will be measured by the GCMS experiment, and indirectly by the SSP experiment².

In the upper atmosphere the physical properties of the atmosphere can be derived from the equation

$$\rho = -\frac{2m}{C_D A} \frac{|\mathbf{a}_{Ad}|}{|\mathbf{v}_{rel}|^2} \quad (24)$$

where m , A and C_D are the probe mass, cross-section area and drag coefficient respectively. Note that m will change along the trajectory due to the heat shield ablation which will be modelled according to Gaborit (2003)

$$m(t) = m_0 \times \exp \left\{ 2\sigma (|\mathbf{v}_{rel}|^2 - |\mathbf{v}_0|^2) \right\} \quad (25)$$

with $\sigma \simeq 4.18 \times 10^{-10} \text{ m}^{-2} \text{ s}^2$ and the initial mass m_0 of 319 kg. \mathbf{v}_0 is the relative velocity of the probe at the time of the start of the ablation process and is taken as the maximum probe velocity. The σ value was chosen to fit the entire ablation mass loss to be 9.7 kg.

For the first iteration the drag coefficient C_D in Eq. (24) is assumed to have a constant value. $|\mathbf{v}_{rel}|$ is known from the numerical integration of the equations of motion and $|\mathbf{a}_{Ad}|$ is derived from the measured accelerations according to Eq. (15). For subsequent iterations a more accurate

²The SSP API-V sensor measures the speed of sound which can be used together with the HASI T measurements to derive the molecular mass from Eq. (19)

value of C_D will be derived by interpolation from a pre-flight aerodynamic database that provides this parameter as a function of Mach number and angle of attack. Note that according to Eq. (14) the derivation of α also requires the knowledge of Ma which implies a second iteration process as outlined in Fig. 2.

Once the density profile is derived the atmospheric pressure p can be derived by integrating the equation of hydrostatic equilibrium

$$p(z) = -\rho(z_0) g \left(\frac{d}{dz} \ln \rho \right)_{z_0}^{-1} - \int_{z_0}^z \rho g dz \quad (26)$$

The temperature T is determined from the ideal gas law with knowledge of the mean molecular weight μ using the relation

$$T(z) = \frac{p(z) \mu}{\rho(z) R} \quad (27)$$

4. REDUNDANT MEASUREMENT DATA

The numerical integration of the measured spacecraft accelerations and the modelled gravitational accelerations provide an initial *reference trajectory* from interface altitude down to the surface. Due to the oscillatory motions of the probe-parachute systems the reference trajectory will most likely deviate to some extent from the real one and must be updated using additional (independent) data sets that provide information on the probe position like the altitude z and the descent speed \dot{z} which will be determined primarily by HASI, the Radar Altimeter Units, and DISR.

4.1. Conversion of HASI P & T Measurements

The reconstruction of the probe altitude during the descent phase is based on the HASI temperature and pressure measurements T and P respectively which can be converted to an altitude z_i at an epoch t_i by:

$$z_i = z_0 - \sum_i \Delta z_{i-1} \quad (28)$$

where z_0 is the initial altitude (i.e., the altitude at which the first pressure measurement was taken) and Δz_i is the distance the probe has travelled in the time interval Δt_i . The equation of state for a real gas can be expressed as

$$\frac{P \mu}{\rho R T} = \zeta \quad (29)$$

where ρ is the gas density, μ the molecular weight, and R the universal gas constant. The compressibility factor

ζ takes into account the non perfect gas behavior and is given by Dymond (1992)

$$\zeta = 1 + \frac{B_{2,M}(T)\rho}{\mu} \equiv 1 + \epsilon \quad (30)$$

where $B_{2,M}$ is the second virial coefficient which for a gas mixture with k species is given by the equation

$$B_{2,M} = \sum_k x_k^2 B_{2,k}(T) + \sum_{k < j} x_k x_j B_{2,k-j}(T) \quad (31)$$

x_k and x_j are the mole fractions of species k and j , $B_{2,k}$ and $B_{2,j}$ are the corresponding second virial coefficients (for pure components), and $B_{2,k-j}$ is the so-called interaction virial coefficient (also referred to as the cross virial coefficient). Note that for calculations at pressures not much greater than 1 atm, a knowledge of the second virial coefficient is usually sufficient, as the contribution of the third virial coefficient will only be significant at very high pressures (Dymond, 1992). Using Eq. (29) and the equation for hydrostatic equilibrium

$$\frac{1}{\rho} \frac{\partial P}{\partial z} = -g, \quad (32)$$

where z is the altitude above the reference surface and g the vertical component of the effective gravitational field, one can derive the following relation for the altitude Δz_i in Eq. (28) (Gaborit, 2004)

$$\Delta z_i = -\frac{RT_{i-\frac{1}{2}}\zeta}{\mu g} \ln\left(\frac{P_i}{P_{i-1}}\right). \quad (33)$$

The subscript i is relative to a value obtained at the mission time t_i and the temperature T is assumed to be constant between times t_{i-1} and t_i having the value $T_{i-\frac{1}{2}} = \frac{1}{2}(T_{i-1} + T_i)$.

To take into account dynamical effects, both the temperature and the pressure data have to be corrected using the two following equations (Gaborit, 2004):

$$T_{stat} = \frac{T_{meas}}{1 + [(\gamma - 1)/2] Ma^2}$$

$$P_{stat} = P_{meas} \left(1 + \frac{\gamma - 1}{2} Ma^2\right)^{\frac{\gamma}{1-\gamma}} \quad (34)$$

where T_{stat} and P_{stat} are the static temperature and pressure values and T_{meas} and P_{meas} the measured ones, and Ma the Mach number. γ is the ratio of the heat capacities of the mixed gas and has to be calculated by

$$\gamma = \frac{f_k C_{p,k}}{f_k C_{p,k} - R} \quad (35)$$

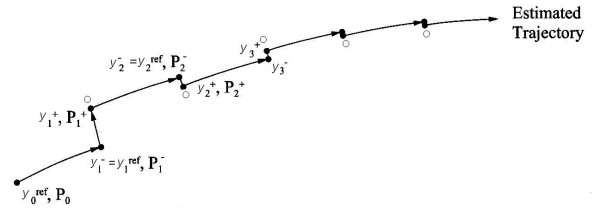


Figure 3. The extended Kalman Filter (EKF) makes use of the latest estimate to propagate the state vectors and the state transition matrix. The white circles represent the measurement vectors m at the various measurement epochs (Montenbruck and Gill, 2000).

f_k and $C_{p,k}$ are the mole fraction and specific heat capacities at constant pressure of species k respectively.

4.2. The Radar Altimeter Units (RAU)

The Proximity Sensor/Radar Altimeter Unit, comprising two completely redundant radar altimeters (unit A, 15.4 to 15.43 GHz and unit B, 15.8 to 15.83 GHz), is responsible for measuring the probe altitude from about 25 km to the surface. Each altimeter transmits a swept frequency modulated continuous wave (FMCW) in which the sweep period is adjusted so that the frequency of the return signal differs by 200 kHz from that of the transmitted signal. Since the transmitted frequency is swept, the sweep period is directly related to the propagation time and, therefore, to altitude. At altitudes above about 25 km the radar operation is limited by noise (low signal levels) and loss of lock and is of doubtful reliability.

4.3. SSP Acoustic Sounder (API-S)

The API-S element of the Surface Science Package will give information on surface roughness and acoustic back-scattering properties of Titan's surface during the last few hundred meters and should provide an accurate measure of the probe altitude and descent velocity (Zarnecki *et al.*, 1997).

4.4. DISR Probe Position Measurements

The DISR Side-Looking, Medium-Resolution and High-Resolution Imager sensor measurements can be processed to provide information on the probe position (latitude, longitude and altitude) and its descent velocity (after differentiating the position vectors) and will be used to further constrain the reference trajectory (Tomasko *et al.*, 1997).

5. FORMULATION OF THE KALMAN FILTER

To take into account the redundant data sets to constrain and update the reference trajectory a sequential estima-

tion algorithm or Kalman filter will be used. A Kalman filter allows one to sequentially use a measurement vector \mathbf{m} given at a measurement epoch t_i to obtain an improved state vector \mathbf{y}_i and the associated covariance matrix \mathbf{P}_i at t_i (see Fig. 3). For a successful application of the basic Kalman filter the deviations between the reference state and the estimated state must be small enough to neglect any non-linearities in the system dynamics and the measurement modeling. In order to avoid this restriction and make full use of the advantages of sequential estimation for trajectory determination purposes the *Extended Kalman Filter* has been developed (Montenbruck and Gill, 2000). The *time update phase* of the extended filter comprises the propagation of the previous estimate \mathbf{y}_{i-1}^+ from t_{i-1} to t_i and the simultaneous solution of the variational equations for the state transition matrix Φ_i . As a result one obtains the predicted state vector \mathbf{y}_i^- and the associated covariance matrix \mathbf{P}_i^- :

$$\begin{aligned} \mathbf{y}_i^- &= \mathbf{y}_{i-1}^+ \\ \mathbf{P}_i^- &= \Phi_i \mathbf{P}_{i-1}^+ \Phi_i^T \end{aligned} \quad (36)$$

Note that the superscript “-” designates the a priori state vector (i.e., the state vector without the information of the additional measurements) and the superscript “+” designates the so called a posteriori or updated state vector. The transition matrix Φ_i at the epoch t_i is given by

$$\Phi_i \equiv \Phi(t_i, t_{i-1}) \equiv \frac{\partial \mathbf{y}_i^{\text{ref}}}{\partial \mathbf{y}_{i-1}^{\text{ref}}} = \Phi(t_i, t_0) \Phi(t_{i-1}, t_0)^{-1} \quad (37)$$

which follows from the definition of the transition matrix

$$\Phi(t_i, t_0) = \begin{pmatrix} \frac{\partial y_1(t_i)}{\partial y_1(t_0)} & \cdots & \frac{\partial y_1(t_i)}{\partial y_6(t_0)} \\ \vdots & \ddots & \vdots \\ \frac{\partial y_6(t_i)}{\partial y_1(t_0)} & \cdots & \frac{\partial y_6(t_i)}{\partial y_6(t_0)} \end{pmatrix} \quad (38)$$

and has to be calculated either by solving the appropriate variational equations or by calculating a difference quotient approximation. The *measurement update phase* is given by:

$$\begin{aligned} \mathbf{K}_i &= \mathbf{P}_i^- \mathbf{G}_i^T \cdot (\mathbf{W}_i^{-1} + \mathbf{G}_i \mathbf{P}_i^- \mathbf{G}_i^T)^{-1} \\ \mathbf{y}_i^+ &= \mathbf{y}_i^- + \mathbf{K}_i \cdot \{\mathbf{m}_i - \mathbf{g}_i(\mathbf{y}_i^-)\} \\ \mathbf{P}_i^+ &= (\mathbf{1} - \mathbf{K}_i \mathbf{G}_i) \cdot \mathbf{P}_i^- \end{aligned} \quad (39)$$

where

$$\mathbf{m}_i = \begin{pmatrix} Z \\ \dot{Z} \end{pmatrix} \Big|_{t=t_i} \quad \text{and} \quad \mathbf{g}_i = \begin{pmatrix} z \\ \dot{z} \end{pmatrix} \Big|_{t=t_i} \quad (40)$$

are the observed and calculated (or modelled) measurement vectors respectively and \mathbf{K}_i is the so called Kalman gain. Here Z and \dot{Z} are the measured altitude and descent speed. \mathbf{G}_i is a Jacobian of the calculated altitude z and descent speed \dot{z} with respect to the reference state vector at the epoch t_i and is given by

$$\mathbf{G}_i = \left(\frac{\partial \mathbf{g}}{\partial \mathbf{y}^{\text{ref}}} \right) \Big|_{t=t_i} = \begin{pmatrix} \partial z / \partial \mathbf{r} & \mathbf{0}_{1 \times 3} \\ \partial \dot{z} / \partial \mathbf{r} & \partial \dot{z} / \partial \mathbf{v} \end{pmatrix} \Big|_{t_i}^{2 \times 6} \quad (41)$$

\mathbf{W} is the weighting matrix at the epoch t_i and can be written as

$$\mathbf{W}_i = \begin{pmatrix} \sigma_Z^{-2} & 0 \\ 0 & \sigma_{\dot{Z}}^{-2} \end{pmatrix} \Big|_{t=t_i} \quad (42)$$

where σ_Z and $\sigma_{\dot{Z}}$ are the 1σ measurement errors of Z and \dot{Z} respectively. The filter starts with an initial guess for the state vector $\mathbf{y}_0 = \mathbf{y}_0^{\text{apr}}$ and the covariance matrix $\mathbf{P}_0 = \mathbf{P}_0^{\text{apr}}$. Due to the regular update of the reference state non-linearities are reduced to a minimum and within a few time steps the filter may arrive at a solution that would otherwise require multiple iterations.

x	-211.6721028
y	-3821.140624
z	-371.6251621
vx	-2.340519721
vy	5.54026603
vz	0.4587518978

Table 1. Huygens probe state vector at interface epoch (UTC JAN 14, 2005 08:58:55.816) in an inertial Titan centered coordinate system (i.e., Earth mean equator and equinox of J2000). (From JPL-020910 Delivery); Units are km and km/s respectively.

6. ALGORITHM TEST CASES AND PRELIMINARY RESULTS

6.1. Reconstruction of the Simulated Huygens Trajectory

The simulated Huygens entry and descent trajectory was used to test the reference trajectory reconstruction component of the algorithm. The trajectory was simulated by the official Huygens mission analysis software (called DTAT) (Belló-Mora and Sánchez-Nogales, 2000) which is able to perform:

- a simulation of the Huygens entry and descent trajectory from the nominal interface point (1270 km altitude) down to the surface and determination of the landing point that will be used as a prediction to

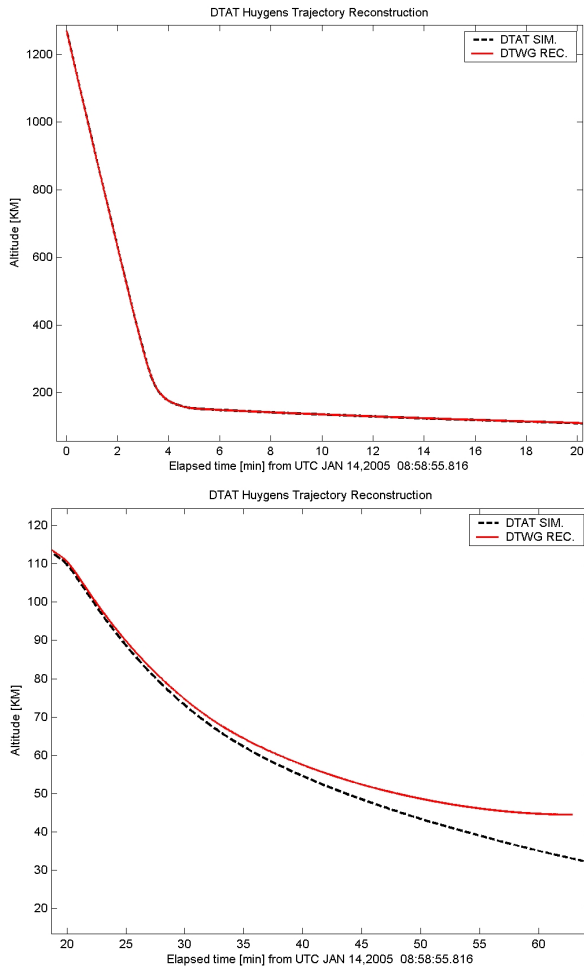


Figure 4. Comparison of DTAT simulated altitude profile (dashed line) and reconstructed profile (solid line). During the first 20 minutes of the mission (upper panel) both trajectories are consistent but the reconstructed trajectory starts to diverge from the simulated one after 20 minutes (lower panel) due to the low sampling output of the simulated aerodynamic accelerations of the DTAT tool.

point the Cassini High Gain Antenna (HGA). The simulation takes into account the Yelle nominal Titan atmosphere model (Yelle *et al.*, 1997) and various versions of the standard Titan wind model basing on Flasar *et al.* (1997). The tool provides the (simulated) accelerations that act on the probe (i.e., central body, third body, solar perturbation, aerodynamic drag) in a separate output file.

- a propagation of the probe navigation covariance matrix (provided by the Cassini Navigation team at interface altitude) down to the surface, which yields the landing dispersion ellipse.
- a statistical (Monte Carlo Methods) simulation of the Cassini/Huygens Probe Relay Link (PRL) during the entire mission.

Two reconstruction efforts have been performed. To test the non aerodynamic force modelling of the algorithm, the first reconstruction of the simulated probe trajectory

x	1360.62662662080
y	-3176.82807430583
z	-679.964270556047
vx	-7.16847147687223
vy	-1.15739189422690
vz	0.205091024784583

Table 2. Mars Pathfinder state vector at the epoch UTC JUL 04, 1997 16:51:50.482 in a Mars centered coordinate system (i.e., Earth mean equator and equinox of J2000). (From JPL-020910 Delivery); Units are km and km/s respectively.

assumed no atmosphere. The second reconstruction used the nominal Yelle Titan atmosphere with no winds. Both reconstruction efforts used the initial conditions as specified in the JPL-020910 delivery file to ESA (see Table 1).

The no atmosphere trajectory implies a probe impact only ~ 240 seconds after interface epoch. The trajectories simulated by the DTAT tool and the DTWG tool fall very close together which clearly shows that all the numerical modelling of the non-aerodynamic forces and the necessary frame transformations have been done correctly. Fig. 4 shows the comparison for the simulation with the nominal Yelle atmosphere. During the first 20 minutes after interface epoch both trajectories are very consistent (see upper panel of Fig. 4) but start to deviate after 20 minutes and finally diverge at about 60 minutes (see lower panel of Fig. 4). The reason for this behavior can be explained by the fact that the sampling output rate of the aerodynamic accelerations of the DTAT tool is too low (average ~ 0.1 Hz), resulting in a constant build up of error which finally leads to a significant divergence of the reconstructed trajectory from the simulated one. Unless the acceleration sampling output rate of the DTAT tool is changed (this would require a modification of the source code) it can serve only to a limited extent as a test bed for the DTWG reconstruction tool.

6.2. The Reconstruction of the Mars Pathfinder Trajectory

The Mars Pathfinder (MPF) spacecraft entered the Martian atmosphere directly from an Earth-to-Mars interplanetary transfer trajectory with an inertial velocity of 7.26 km/s (Golombek *et al.*, 1999). The spacecraft EDL (Entry, Descent, and Landing) strategy comprised the use of an aeroshell (i.e., forebody heatshield and aftbody backshell) during the entry phase, a parachute for the descent phase, a set of three solid rockets, a radar altimeter unit, and an airbag system for the final part of the descent and the impact on the surface. Two sets of three orthogonally-positioned Allied Signal QA-3000 accelerometers each provided 2-axis acceleration measurements during entry. One set of accelerometers was part of the Atmospheric Structure Investigation/Meteorology (ASI/MET) experiment (Schofield *et al.*, 1997; Seiff *et al.*, 1997), which were range switched during the entry trajectory to provide increased resolution. The ASI/MET accelerometers were aligned parallel to the entry vehicle coordinate axes.

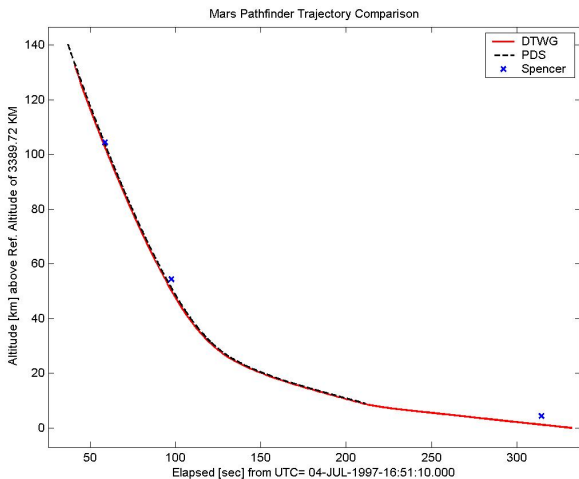


Figure 5. Comparison of altitude profiles for the Mars Pathfinder mission. The solid line represents the reconstructed trajectory from the DTWG algorithm which is compared to the PDS archived trajectory (dashed line) from Magalhães *et al.* (1999) and three points of the reconstructed profile by Spencer *et al.* (1998).

The ASI/MET accelerometer measurements and the reconstructed trajectory together with the derived atmospheric properties are available on the PDS volume MPAM_0001 which is online at

http://atmos.nmsu.edu/PDS/data/mpam_0001/.

The reconstruction effort that corresponds to the PDS archived trajectory and atmosphere is documented in Magalhães *et al.* (1999). An independent reconstruction effort was done by Spencer *et al.* (1998) and was based on the combination of accelerometer, altimeter, and ground-based measurements of received frequency using sequential filtering and smoothing techniques. Note that both efforts used different initial conditions (i.e., a different initial altitude). In our work we used the initial conditions as provided by Spencer *et al.* (1998) and converted them into a Mars EME2000 reference system (see Table 2).

Fig. 5 shows a comparison of the altitude profile of the three reconstruction efforts, the PDS archived trajectory (dashed line), the DTWG trajectory (solid line), and finally three data points from the Spencer *et al.* (1998) trajectory. It is important to note that both the PDS and DTWG altitude profile were directly calculated with respect to the radius of the MPF landing site of 3389.72 km (Golombek *et al.*, 1997), whereas the Spencer altitude profile was given with respect to the Mars reference ellipsoid and had to be converted³ accordingly for the comparison in Fig. 5. The altitude residuals between the PDS and DTWG profiles decrease from 1.2 km at the beginning of the entry phase to only 0.25 km in the final part of the descent. The altitude difference of the last data point by Spencer *et al.* (1998) and the DTWG trajectory is about 3 km, which very likely is due to the fact that the DTWG reconstruction effort so far is based only

³The rotational ellipsoid with A=3396.19 km and B=3376.20 km as reported by Duxbury (2002) was assumed for the conversion.

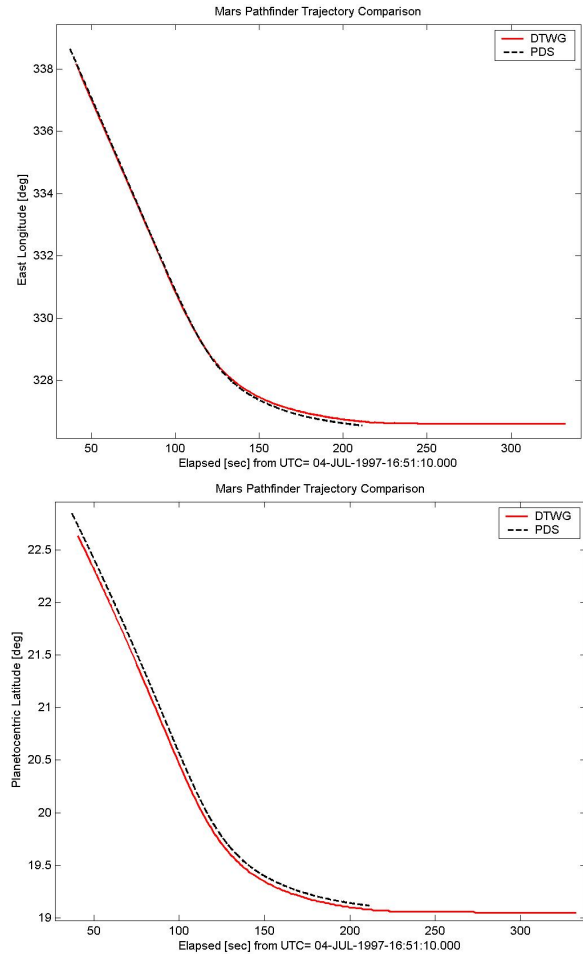


Figure 6. Comparison of the Mars Pathfinder East longitude profile (upper panel) and the latitude profile (lower panel) of the DTWG reconstructed trajectory (solid line) and the PDS archived trajectory as reported by Magalhães *et al.* (1999) (dashed line).

on the measured aerodynamic accelerations, whereas the Spencer trajectory also takes into account measurements of the Radar Altimeter Unit and groundbased frequency measurements.

Fig. 6 shows a comparison of the latitude and longitude profiles of the PDS and DTWG trajectories (no such profiles were provided in the Spencer *et al.* (1998) publication). Table 3 compares the MPF landing point coordinates of the DTWG reconstructed trajectory to the coordinates obtained by Magalhães *et al.* (1999), by landmark recognition and lander radiometric tracking (Golombek *et al.*, 1997). One can see that the differences in all cases are lower than 0.2 deg in longitude and 0.3 deg in latitude.

The atmospheric properties were reconstructed according to Eqs. (24-27). During the entry phase, the total mass of the Mars Pathfinder entry vehicle was $m = 585.3$ kg and its area was $A = 5.526$ m². The drag coefficient of the probe varies during the entry, and this variation was accounted for iteratively using the aerodynamic database from Moss *et al.* (1998). The drag coefficient was interpolated as function of the angle of attack α and hard sphere Knudsen number $Kn_{\infty,HS}$ and is shown in Fig. 7.

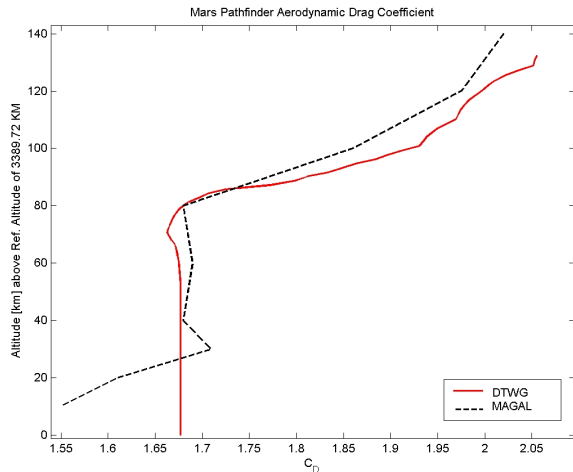


Figure 7. Comparison of interpolated drag coefficient C_D with the corresponding profile published in Fig. 3 of Magalhães et al. (1999)

Method	E. Long. [deg]	Latitude [deg]
DTWG reconstr.	326.62	19.05
Landmark Recogn.	326.45	19.33
Radiom. Tracking	326.48	19.28
PDS Archive	326.48	19.09

Table 3. Comparison of reconstructed MPF landing point (with initial conditions from Table 2) and landing point coordinates derived from independent methods.

Figures 8 and 9 show the DTWG reconstructed atmospheric profiles (solid line) and compares them to the corresponding profiles as archived in the PDS (dashed lines). Both the DTWG reconstructed trajectory and the atmospheric properties are consistent with the results from the previous efforts. The observed residuals arise from the slightly different coefficients in the aerodynamic database used in the reconstruction procedures.

6.3. The Huygens Simulated Dataset

An extensive effort is devoted to the preparation of a synthetic dataset that is representative of all the measurement parameters of the various Huygens instruments contributing to the DTWG reconstruction effort (Pérez-Ayúcar *et al.*, 2003). This dataset will serve as the main test bed for the final implementation of the full reconstruction algorithm. The simulated dataset will be derived from the results of the DTAT tool, the PASDA tool (a high fidelity model of the probe that provided the attitude variations in response to various disturbances), and a 5 DOF tool providing the prediction of the angular body rates during the probe entry.

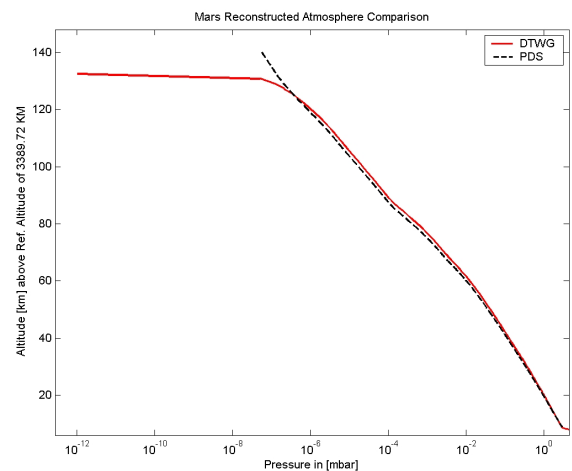
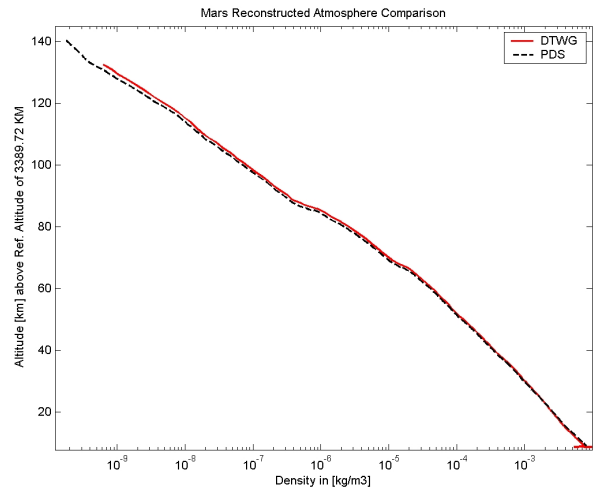


Figure 8. Comparison of the reconstructed density, pressure and temperature profile (upper and lower panel respectively) of the Mars atmosphere from MPF aerodynamics accelerations during the entry phase.

7. CONCLUSION

The ESA Huygens probe with a suite of six instruments will enter the atmosphere of Titan in January, 2005. For the correct scientific interpretation and correlation of the different measurements a single and common entry and descent profile is needed that is consistent with all available probe science and engineering data. The Huygens Descent Trajectory Working Group is developing and implementing an algorithm that will reconstruct the Huygens entry and descent trajectory on the basis of the various instrument and housekeeping measurements. The tool will combine standard techniques of entry probe accelerometry with a Kalman filtering technique to ensure the best combination and maximum consistency of all the used experiment data. The accelerometer reconstruction part of the algorithm was successfully tested with the simulated trajectory and accelerometer measurement output of the official Huygens mission analysis software DTAT and furthermore with the archived ASI/MET science accelerometer measurements of the Mars Pathfinder spacecraft. The development of a synthetic Huygens dataset will provide a testbed prior to the final implementation of

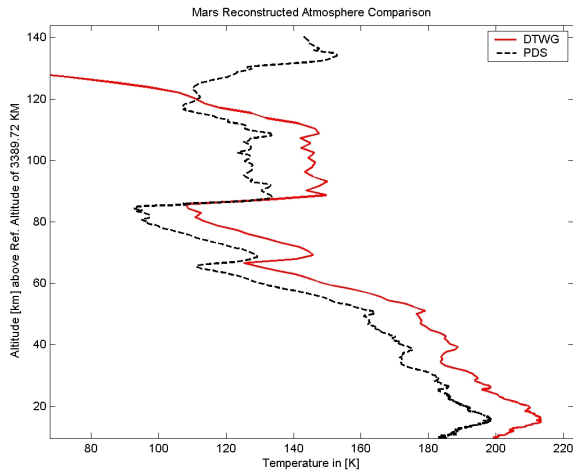


Figure 9. Comparison of the reconstructed temperature profile of the Mars atmosphere from MPF aerodynamics accelerations during the entry phase.

the full DTWG trajectory reconstruction code.

8. ACKNOWLEDGEMENTS

The authors thank the European Space Agency for support via the Descent Trajectory Working Group investigation. We thank Vincent Gaborit and Paul Withers for valuable comments.

REFERENCES

- ATKINSON, D. 1998. Report of the Huygens Descent Trajectory Working Group. Technical report, University of Idaho.
- BELLÓ-MORA, M., AND M. SÁNCHEZ-NOGALES 2000. Huygens Entry and Descent Software Development Final Report. Technical Report GMV-HUYGENS-FR, GMV.
- BIRD, M. K., M. HEYL, M. ALLISON, W. ASMAR, D. ATKINSON, P. EDENHOFER, D. PLETTEMEIER, R. WOHLMUTH, L. IESS, AND G. L. TYLER 1997. The Huygens Doppler Wind Experiment. In *Huygens: Science, Payload and Mission*, pp. 139+.
- DUXBURY, T. C. 2002. MARS GEODESY/CARTOGRAPHY WORKING GROUP RECOMMENDATIONS ON MARS CARTOGRAPHIC CONSTANTS AND COORDINATE SYSTEMS. In *ISPRS WG IV/9: Extraterrestrial Mapping Workshop*. Online at: <http://astrogeology.usgs.gov/Projects/ISPRS/MEETINGS/ottawa/>.
- DYMOND, J. H. 1992. *The Virial Coefficients of Pure Gases and Mixtures, a Critical Compilation*. Oxford University Press, Oxford.
- FLASAR, F. M., M. D. ALLISON, AND J. I. LUNINE 1997. Titan Zonal Wind Model. In *Huygens: Science, Payload and Mission*, pp. 287+.
- FULCHIGNONI, M., F. ANGRILLI, G. BIANCHINI, A. BAR-NUN, M. A. BARUCCI, W. BORUCKI, M. CORADINI, A. COUSTENIS, F. FERRI, R. J. GRARD, M. HAMELIN, A. M. HARRI, G. W. LEPPELMEIER, J. J. LOPEZ-MORENO, A. M. McDONNELL, C. MCKAY, F. M. NEUBAUER, A. PEDERSEN, G. PICARDI, V. PIRRONELLO, R. PRIJOLA, R. RODRIGO, C. SCHWINGENSCHUH, A. SEIFF, H. SVEDHEM, E. THRANE, V. VANZANI, G. VISKONTI, AND J. ZARNECKI 1997. The Huygens Atmospheric Structure Instrument. In *Huygens: Science, Payload and Mission*, pp. 163+.
- GABORIT, V. 2003. *Modèles et méthodes expérimentales qui supportent une mission spatiale: reconstruction de la trajectoire d'une sonde dans atmposphère planétaire*. Ph. D. thesis, Université de Paris VII Jussieu.
- GABORIT, V. 2004. Procedure Development for the Trajectory Reconstruction of a Probe Descending in a Planetary Atmosphere: Application to Galileo and HASI ballon tests. In *ESA SP-544: Planetary Probe Atmospheric Entry and Descent Trajectory Analysis and Science (this issue)*.
- GOLOMBEK, M. P., R. C. ANDERSON, J. R. BARNES, J. F. BELL, N. T. BRIDGES, D. T. BRITT, J. BRÜCKNER, R. A. COOK, D. CRISP, J. A. CRISP, T. ECONOMOU, W. M. FOLKNER, R. GREELEY, R. M. HABERLE, R. B. HARGRAVES, AND ET AL. 1999. Overview of the Mars Pathfinder Mission: Launch through landing, surface operations, data sets, and science results. *Journal of Geophysical Research* **104**, 8523–8554.
- GOLOMBEK, M. P., R. A. COOK, T. ECONOMOU, W. M. FOLKNER, A. F. C. HALDEMANN, P. H. KALLEMEYN, J. M. KNUDSEN, R. M. MANNING, H. J. MOORE, T. J. PARKER, R. RIEDER, J. T. SCHOFIELD, P. H. SMITH, AND R. M. VAUGHAN 1997. Overview of the Mars Pathfinder Mission and Assessment of Landing Site Predictions. *Science* **278**, 1743–+.
- ISRAEL, G., H. NIEMANN, F. RAULIN, W. RIEDLER, S. ATREA, S. BAUER, M. CABANE, E. CHASSEFIÈRE, A. HAUCHECORNE, T. OWEN, C. SABLÉ, R. SAMUELSON, J. P. TORRE, C. VIDAL-MADJAR, J. F. BRUN, D. COSCIA, R. LY, M. TINTIGNAC, M. STELLER, C. GELAS, E. CONDÉ, AND P. MILAN 1997. The Aerosol Collector Pyrolyser Experiment for Huygens. In *Huygens: Science, Payload and Mission*, pp. 59+.
- LEBRETON, J.-P., AND D. L. MATSON 2002. The Huygens Probe: Science, Payload and Mission Overview. *Space Science Reviews* **104**, 59–100.
- MAGALHÃES, J. A., J. T. SCHOFIELD, AND A. SEIFF 1999. Results of the Mars Pathfinder atmospheric structure investigation. *Journal of Geophysical Research* **104**, 8943–8956.
- MONTENBRUCK, O., AND E. GILL 2000. *Satellite Orbits: Models, Methods, Application*. Berlin ; New York : Springer, c2000.
- MOSS, J., R. C. BLANCHARD, R. G. WILMOTH, AND R. D. BRAUN 1998. Mars Pathfinder Rarefied Aerodynamics: Computations and Measurements. *AIAA 98-0298*.

- NIEMANN, H., S. ATREYA, S. J. BAUER, K. BIEMANN, B. BLOCK, G. CARIGNAN, T. DONAHUE, L. FROST, D. GAUTIER, D. HARPOLD, D. HUNTEN, G. ISRAEL, J. LUNINE, K. MAUERSBERGER, T. OWEN, F. RAULIN, J. RICHARDS, AND S. WAY 1997. The Gas Chromatograph Mass Spectrometer Aboard Huygens. In *Huygens: Science, Payload and Mission*, pp. 85+.
- PÉREZ-AYÚCAR, M., O. WITASSE, J. P. LEBRETON, B. KAZEMINEJAD, AND D. H. ATKINSON 2003. A Simulated Dataset of the Huygens Mission. In *ESA SP-544: Planetary Probe Atmospheric Entry and Descent Trajectory Analysis and Science (this issue)*.
- SCHOFIELD, J. T., J. R. BARNES, D. CRISP, R. M. HABERLE, S. LARSEN, J. A. MAGALHAES, J. R. MURPHY, A. SEIFF, AND G. WILSON 1997. The Mars Pathfinder Atmospheric Structure Investigation/Meteorology. *Science* **278**, 1752+.
- SEIFF, A., J. E. TILLMAN, J. R. MURPHY, J. T. SCHOFIELD, D. CRISP, J. R. BARNES, C. LABAW, C. MAHONEY, J. D. MIHALOV, G. R. WILSON, AND R. HABERLE 1997. The atmosphere structure and meteorology instrument on the Mars Pathfinder lander. *Journal of Geophysical Research* **102**, 4045–4056.
- SPENCER, D. A., R. C. BLANCHARD, S. W. THURMANN, R. D. BRAUN, C.-Y. PENG, AND P. H. KALLEMEYN 1998. Mars Pathfinder Atmospheric Entry Reconstruction. Technical Report AAS 98-146, NASA.
- STEINER, G., AND S. J. BAUER 1990. Molecular and eddy diffusion in the atmosphere of Titan. *Annales Geophysicae* **8**, 473–476.
- STROBEL, D. F., M. E. SUMMERS, AND X. ZHU 1992. Titan's upper atmosphere - Structure and ultraviolet emissions. *Icarus* **100**, 512–526.
- TOMASKO, M. G., L. R. DOOSE, P. H. SMITH, R. A. WEST, L. A. SODERBLOM, M. COMBES, B. BÉZARD, A. COUSTENIS, C. DEBERGH, E. LELLOUCH, J. ROSENQVIST, O. SAINT-PÉ, B. SCHMITT, U. H. KELLER, N. THOMAS, AND F. GLIEM 1997. The Descent Imager/spectral Radiometer Aboard Huygens. In *Huygens: Science, Payload and Mission*, pp. 109+.
- YELLE, R. V., D. F. STROBEL, E. LELLOUCH, AND D. GAUTIER 1997. The Yelle Titan Atmosphere Engineering Models. In *Huygens: Science, Payload and Mission*, pp. 243+.
- ZARNECKI, J. C., M. BANASZKIEWICZ, M. BANNISTER, W. V. BOYNTON, P. CHALLENGER, B. CLARK, F. M. DANIELL, J. DELDERFIELD, M. A. ENGLISH, M. FULCHIGNONI, J. R. C. GARRY, J. E. GEAKE, S. F. GREEN, B. HATHI, S. JAROSLAWSKI, M. R. LEESE, R. D. LORENZ, J. A. M. MCDONNELL, N. MERRYWEATHER-CLARKE, C. S. MILL, R. J. MILLER, G. NEWTON, D. J. PARKER, P. RABBETTS, H. SVEDHEM, R. F. TURNER, AND M. J. WRIGHT 1997. The Huygens Surface Science Package. In *Huygens: Science, Payload and Mission*, pp. 177+.